IJMGE, Vol.50, No.2, (2016) 231–238

International Journal of Mining and Geo-Engineering

Hybrid ANFIS with ant colony optimization algorithm for prediction of shear wave velocity from a carbonate reservoir in Iran

H. Fattahi [a*], H. Nazari [a], A. Molaghab [b]

[a] *Department of Mining Engineering, Arak University of Technology, Arak, Iran*
[b] *National Iranian South Oil Company, Ahvaz, Iran*

ARTICLE HISTORY

Received 12 May 2016, Received in revised form 30 Sep 2016, Accepted 01 Oct 2016

ABSTRACT

Shear wave velocity (V_s) data are key information for petro-physical, geophysical and geomechanical studies. Although compressional wave velocity (V_p) measurements are available in almost every well, shear wave velocity is usually not recorded for most of old wells due to the technological limitations. Furthermore, measurement of shear wave velocity comparatively costly. This study proposes a novel methodology to tackle these problems by taking advantage of Hybrid Adaptive Neuro Fuzzy Inference System (ANFIS) with Ant Colony Optimization algorithm (ACO) based on Fuzzy C–Means Clustering (FCM) and Subtractive Clustering Method (SCM). The ACO is combined with two ANFIS models for determination of the optimal value of its user–defined parameters. The optimization implementation by the ACO significantly improves the generalization ability of the ANFIS models. These models are used in this study to formulate conventional well log data into V_s in a swift, economical, and accurate manner. A total of 3030 data points were used for model construction and 833 data points were employed for assessment of ANFIS models. Finally, a comparison among ANFIS models, and six well–known empirical correlations proved that ANFIS models can outperform the other methods. This strategy was successfully applied in the Marun reservoir, Iran.

Keywords: *Shear wave velocity; Carbonate reservoir; ANFIS-subtractive clustering; ANFIS-fuzzy c–means clustering; Ant colony optimization algorithm*

1. Introduction

Shear wave velocity (V_s) is an important parameter, which has many applications in reservoir characterization and geomechanical studies. V_s can provide invaluable data for reservoir study such as rock mechanical properties calculation of, lithology identification [1], and pore type identification [2]. True measurement of this parameter, carried out by dipole sonic imager or laboratory measurements, is very expensive. Therefore, many researchers have attempted to find rapid and accurate alternative ways to predict this parameter. Intelligent methods such as artificial neural networks (ANN), fuzzy systems (FS), swarm intelligence (SI) and evolutionary algorithms (EA) are robust tools for estimation of this parameter. Review of the literature shows that many intelligent methods for prediction of V_s have been suggested by the past researchers. In this paper, these well–known research works are addressed. H. Eskandari et al used multiple regression and artificial neural network techniques to predict shear wave velocity from wireline log data for a carbonate reservoir, south-west Iran [3]. M. R. Rezaee et al. utilized intelligent systems for prediction of shear wave velocity from petrophysical data [4]. M. Rajabi et al. proposed intelligent approaches for prediction of compressional, shear and stoneley wave velocities from conventional well log data [5]. I. Moatazedian et al. used genetic algorithms technique for prediction of shear and compressional wave velocities from petrophysical data [6]. M. Asoodeh, P. Bagheripour utilized committee machine with intelligent systems for prediction of compressional, shear, and stoneley wave velocities from conventional well log data [7]. P. Bagheripour et al. proposed support vector regression approach for prediction of shear wave velocity [8].

In this study, V_s is estimated from conventional well log data using hybrid adaptive neuro fuzzy inference system (ANFIS) with Ant Colony Optimization Algorithm (ACO) based on Fuzzy C–Means clustering (FCM) and Subtractive Clustering Method (SCM). The ACO is combined with two ANFIS models (ANFIS–FCM and ANFIS–SCM) for determining the optimal value of its user–defined parameters. The optimization implementation by the ACO significantly improves the generalization ability of the ANFIS models. ANFIS–ACO models were compared with six well-known empirical correlations. Results confirm

* Corresponding author.
E-mail address: h.fattahi@arakut.ac.ir (H. Fattahi).

DOI: 10.22059/ijmge.2016.59874
Journal Homepage: ijmge.ut.ac.ir

superiority of ANFIS–ACO models over other methods. This methodology was successfully implemented to Asmari carbonate reservoir rocks, the major reservoir of Iranian Oil Fields. Top of the reservoir formation is varied in range of 2107m to 2769m in the scope of this study.

2. Theory and Methodology

The idea behind the proposed predictor is to optimize values of the ANFIS models using search algorithm. In this section, the ANFIS models is first explained and then followed by describing the employed optimization algorithm of ACO.

2.1. Adaptive Network-based Fuzzy Inference System

An adaptive neural network is a network structure consisting of several nodes connected through directional links. Each node is characterized by a node function with fixed or adjustable parameters. Once the fuzzy inference system (FIS) is initialized, neural network (NN) algorithms can be utilized to determine the unknown parameters (premise and consequent parameters of the rules) minimizing the error measure, as conventionally defined for each variable of the system. Due to this optimization procedure the system is called adaptive [9].

The architecture of ANFIS consists of five layers, and a brief introduction of the model is as follows.

Layer 1: each node *i* in this layer generates a membership grades of a linguistic label. For instance, the node function of the i^{th} node might be:

$$Q_i^1 = \mu_{Ai}(x) = \frac{1}{1+\left[\left(\frac{x-v_i}{\sigma_i}\right)^2\right]^{b_i}} \tag{1}$$

Where, x is the input to node i, and Ai is the linguistic label (small, large...) associated with this node; and $\{\sigma_i, V_i, b_i\}$ is the parameter set that changes the shape of the membership function (MF). Parameters in this layer are referred to as the "premise parameters".

Layer 2: Each node in this layer calculates the "firing strength" of each rule via multiplication:

$$Q_i^2 = W_i = \mu_{Ai}(x).\mu_{Bi}(y) \qquad i = 1,2 \tag{2}$$

Layer 3: The i^{th} node of this layer calculates the ratio of the i^{th} rule's firing strength to the sum of all rules' firing strengths:

$$Q_i^3 = \bar{W}_i = \frac{w_i}{\sum_{j=1}^{2} w_j}, \qquad i = 1,2 \tag{3}$$

For convenience, outputs of this layer will be called "normalized firing" strengths.

Layer 4: Every node *i* in this layer is a node function:

$$Q_i^4 = \bar{W}_i f_i = \bar{W}_i (p_i x + q_i y + r_i) \tag{4}$$

Where, $\bar{W}_i$ is the output of layer #3. Parameters in this layer will be referred to as "consequent parameters".

Layer 5: The single node in this layer is a circle node labeled R that computes the "overall output" as the summation of all incoming signals:

$$Q_i^5 = Overall\ Output = \sum \bar{W}_i f_i = \frac{\sum w_i f_i}{\sum w_i} \tag{5}$$

For a given data set, different ANFIS models can be constructed, using different identification methods. SCM and FCM are two methods used in this study to identify the antecedent MFs.

2.2. Subtractive Clustering Method (SCM)

The SCM is introduced by S. L. Chiu [10] in which data points are considered as the candidates for center of clusters. The algorithm continues as follow:

At first a collection of n data points $\{X_1, X_2, X_3, ..., X_n\}$ in an M-dimensional space is considered. Since each data point is a candidate for cluster center, a density measure at data point X_i is defined as:

$$D_i = \sum_{j=1}^{n} \exp\left(-\frac{\|x_i - x_j\|^2}{\left(\frac{r_a}{2}\right)^2}\right) \tag{6}$$

Where, r_a is a positive constant. Therefore, a data point will have a high density value if it has many neighboring data points. The radius r_a defines a neighborhood; data points outside this radius contribute only slightly to the density measure. After the density measure of each data point has been calculated, the data point with the highest density measure is selected as the first cluster center. Let X_{c1} be the point selected and D_{c1} as its density measure. Next, the density measure for each data point X_i is revised as follows:

$$D_i = D_i - D_{ci} \exp\left(-\frac{\|x_i - x_{ci}\|^2}{\left(\frac{r_b}{2}\right)^2}\right) \tag{7}$$

Where, r_b is a positive constant. After the density calculation for each data point is revised, the next cluster center X_{c2} is selected and all of the density calculations for data points are revised again. This process is repeated until a sufficient number of cluster centers are generated.

By using SCM, the cluster center of all data was found out. Then the numbers of subtractive centers were utilized to generate automatic MFs and rule base, as well as the location of MF within dimensions. This method is a fast clustering method designed for high-dimension problems with a moderate number of data points.

2.3. Fuzzy C-Means Clustering Method

The FCM was originally introduced by J. C. Bezdek [11]. FCM clustering can be viewed as an optimization problem that tries to optimize the following objective function:

$$J_{FCM} = \sum_{i=1}^{C} \sum_{j=1}^{n} u_{ij}^m d_{ij}^2 , \tag{8}$$

where C is the number of clusters, $u_{ij} \in [0,1]$ expresses the membership degree of the data point x_j belonging to the i^{th} fuzzy group, $d_{ij} = \|w_i - x_j\|$ is the Euclidean distance between the i^{th} cluster center w_i and j^{th} data point x_j, and $m \in (1,\infty)$ is a weighting exponent that influences the fuzziness of the clusters.

The FCM starts with an initial guess for the cluster centers, which is intended to mark the mean location of each cluster. The initial guess for these cluster centers will most likely be incorrect. Additionally, the FCM assigns every data point a membership grade for each cluster. By iteratively updating the cluster centers and the membership grades for each data point, the FCM iteratively moves the cluster centers to the "right" location within a data set. This iteration is based on minimizing an objective function that represents the distance from any given data point to a cluster center weighted by the membership grade of that data point. The FCM algorithm is implemented by the following steps:

1. Choose the number of clusters C.
2. Choose *m*, $1 < m < \infty$.
3. Choose a precision for termination ε.
4. Initialize the fuzzy C-partition $U^{(0)}$.
5. Set the iteration counter *t=1*.

6. Update the centers using:

$$w_i = \frac{\sum_{j=1}^{n} \left(u_{ij}^*\right)^m x_j}{\sum_{j=1}^{n} \left(u_{ij}^*\right)^m} \quad for \;\; 1 \le i \le C.$$

7. Update the memberships of all feature vectors in all the clusters using

$$if \;\; \left\| x_j - w_k \right\| = 0 \;\; then \;\; u_{kj}^* = 1 \; and \; u_{kj}^* = 0 \;\; (for \; i \ne k)$$

$$if \;\; \left\| x_j - w_k \right\| \ne 0 \;\; then \;\; u_{ij}^* = \left[\sum_{k=1}^{C} \frac{\left\| x_j - w_i \right\|^{2/(m-1)}}{\left\| x_j - w_k \right\|^{2/(m-1)}} \right]^{-1}.$$

8. If $\left| U^{(t+1)} - U^{(t)} \right| \Leftarrow \varepsilon$ then stop or else t =t+1, go to step 6.

2.4. Ant Colony Optimization Algorithm

The ACO algorithm is an algorithm inspired by real ants. This algorithm was first proposed by Dorigo and colleagues as a novel nature-inspired method for the solution of Combinatorial Optimization (CO) problems in the early 1990s [12]. From then on, researchers have successfully applied the ACO to many optimization problems such as continuous optimization problems [13], global optimum function [14], feature selection [15]. The principle of the method is based on the way ants search for food and find their way back to the nest. Ants can find the shortest path to food by laying a pheromone (chemical) trail as they walk. Other ants follow the pheromone trail to food. Ants that happen to pick the shorter path will create a strong trail of pheromone faster than the ones choosing a longer path. Since stronger pheromone attracts ants more strongly, more and more ants choose the shorter path until eventually all ants have found the shortest path [16].

In the ACO, artificial ants find solutions starting from a start node and moving to feasible neighbor nodes in the process of building the solutions. Each ant builds a tour by frequently applying a stochastic greedy rule, which is called the state transition rule;

$$P(r,u) = \begin{cases} \arg\max_{u \in J(r)} \left\{ \left[\tau(r,u)\right]^{\alpha} . \left[\tau(r,u)\right]^{\beta} \right\}, & if \;\; q \le q_0 \\ S \qquad\qquad , & otherwise \end{cases} \tag{9}$$

(r,u) represents an edge between point *r* and *u*, and $\tau(r,u)$ stands for the pheromone on edge *(r,u)*. $\eta(r,u)$ is the desirability of edge *(r,u)*, which is usually defined as the inverse of the length of edge *(r,u)*. *b* is the parameter controlling the relative importance of the desirability, q_0 is a user-defined parameter with $0 \le q_0 \le 1$, *q* is a random number uniformly distributed in [0, 1]. *J(r)* is the set of edges available at decision point *r*. *S* is a random variable selected according to the probability distribution given below;

$$P(r,s) = \begin{cases} \dfrac{\left[\tau(r,u)\right]^{\alpha} . \left[\tau(r,u)\right]^{\beta}}{\sum_{u \in J(r)} \left[\tau(r,u)\right]^{\alpha} . \left[\tau(r,u)\right]^{\beta}}, & if \;\; s \in J(r) \\ 0 \qquad\qquad , & otherwise \end{cases} \tag{10}$$

While constructing its tour, an ant will modify the amount of the pheromone on the passed edges by applying the local updating rule;

$$\tau(r,s) \leftarrow (1-\rho).\tau(r,s) + \rho\tau_0 \tag{11}$$

Where ρ is the coefficient representing pheromone evaporation, $0 < \rho < 1$.

Once all ants have arrived at their destination, the amount of pheromone on the edge is modified again by applying the global updating rule;

$$\tau(r,s) \leftarrow (1-\delta).\tau(r,s) + \Delta\tau(r,s) \tag{12}$$

Where;

$$\Delta\tau(r,s) = \begin{cases} 1/L_{gb}, & if \; (r,s) \in global \; best \; tour \\ 0 \;\; , & otherwise \end{cases} \tag{13}$$

L_{gb} denotes the length of the globally best tour from the beginning of the trial; the δ is the global pheromone decay parameter, $0 < \delta < 1$ and the $\Delta\tau(r,s)$ is used to increase the pheromone on the path of solution [17].

In this paper, the proposed approach consists of two main steps. First, well log data are prepared to train and test ANFIS models to represent the objective function. Finally, an ACO algorithm is utilized to obtain the optimal objective value. Figure 1 demonstrates the algorithm process of the selection of the ANFIS model parameters based on ACO.

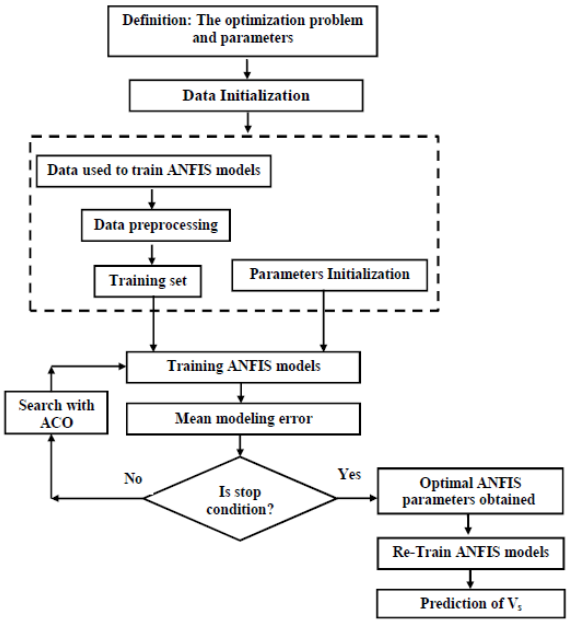

Figure 1. The process of optimizing ANFIS parameters with the ACO.

3. Field Overview

The Marun oil field produces oil from Asmari formation which is a massive carbonate rock, and the structure is 63 km long in the NE–SW direction and 7 km wide. This field is located southeast of the city of Ahwaz in Khuzestan province, southwester Iran. In this field, 48 wells out of a total of 267 wells drilled in Gachsaran formation have experienced collapse, while passing through the sequence of anhydrite, marl and salt layers. Gachsaran is the formation above Asmari, which due to its composition acts as the cap rock. The Gachsaran formation consists of seven members which were deposited one after the other after the deposition of Asmari reservoir formation. Member 1, which is often called cap rock, consists of multiple sequences of anhydrite layers, gray marl layers, thin layers of carbonate and thin layers of dark bituminous to red shale. Up to 75% of this member is made up of anhydrite. Member 2 mainly includes salt layers with cross-bedded layers of anhydrite and gray marl. More than 70% of this member is made up of salt. Anhydrite, gray marl and cross-bedded carbonate are the main layers of member 3. Member 4 is composed of thick layers of salt, gray marl and thin layers of anhydrite; member 5 comprises anhydrite, gray marl and cross-bedded salt and carbonate layers. Member 6 consists of a sequence of anhydrite, red marl and cross-bedded salt layers. Member 7 is composed of anhydrite, gray marl and sometimes cross-bedded carbonate [18,19]. A total of 4163 data points from Asmari formation that have V_s, as measured using the Schlumberger DSI tool, and well log data were used in this study.

4. Inputs and Output Data

Input selection is done to find the strongest inputs for predicting a target. To select the appropriate inputs, conventional well logs that have a logical relationship with V_s are desired. The V_s depends on many factors, which are listed in Table 1 [20,7].

Table 1. List of the parameters that control V_s [20,7].

Environment	Fluid	Rock
Reservoir pressure	Saturation	Pore shape
Geometry of layer	Gas to oil ratio	Porosity
Production history	Fluid type	Fracturing
Reservoir	Hydrophilic	Isotropy
Processes	Fluid phase	Clay content
Temperature	Viscosity	Bulk density
Stress history		Texture
Frequency		Cementation
		Lithification
		History
		Compaction

In this paper, according to the correlation matrix (Table 2), four input parameters including Log Gamma (GR), V_p, vertical stress (σ_v) and bulk density (RHOB), output including V_s were used. Also, it was aimed to model the simplest way for formulating conventional well log data to V_s. Knowing that conventional well logs implicitly record effects of lithology changes, lithology was not used as an input. Several studies which have been done to show conventional well log data contain invaluable lithology information in their records [21,22,8]. In ANFIS-ACO modeling, a dataset that includes 4163 data points was employed in current study, while 3349 data points (80%) were utilized for constructing the models and the remainder data points (870 data points) were utilized for model performance evaluation. Partial dataset used in this study for constructing the ANFIS-ACO models are shown in Table 3. Also, descriptive statistics of the data sets used for modeling are shown in Table 4.

Table 2. Correlation matrix between V_s and independent variables.

	V_s	Log Gamma (GR)	V_p	Drilling Rate (DR)	Vertical Stress (σ)	Bulk Density (RHOB)
V_s	1					
Log Gamma (GR)	-0.6379	1				
V_p	0.8157	-0.7792	1			
Drilling Rate (DR)	-0.0161	-0.2597	0.0008	1		
Vertical Stress (σ)	0.1790	-0.0282	0.1725	0.0414	1	
Bulk Density (RHOB)	0.4014	-0.1250	0.4360	-0.6515	0.0206	1

5. Pre-processing of Data

In data-driven system modeling methods, in order to eliminate any outliers (missing values or bad data), some pre-processing steps are commonly implemented prior to embarking on any calculations. This step ensures that the raw data retrieved from database is perfectly suitable for modeling. In order to soften the training procedure and improving the accuracy of prediction, all data samples are normalized to adapt to the interval [-1, 1] according to the following linear mapping function:

$$x_M = 2\left(\frac{x - x_{\min}}{x_{\max} - x_{\min}}\right) - 1 \quad (14)$$

Where x is the original value from the dataset, x_M is the mapped value, and x_{min} (or x_{max}) denotes the minimum (or maximum) raw input values, respectively. It is to be noted that model outputs will be remapped to their corresponding real values by the inverse mapping function ahead of calculating any performance criterion.

Table 3. Partial dataset used in this study for construction of the models.

No.	Input parameters				Output parameter
	GR	V_p (Km/s)	σ_v (Mpa)	RHOB (kg/m^3)	V_s (Km/s)
1	35.0966	2.62360	54.3679	3191.90	2.2828
2	35.8456	2.61850	54.3718	3191.90	2.2942
3	35.6576	2.61402	54.3757	3191.90	2.3057
4	35.9701	2.60384	54.3796	3191.90	2.3173
5	36.8902	2.59120	54.3835	3191.90	2.3409
6	37.0557	2.62940	54.3874	3191.90	2.3650
7	36.2179	2.68686	54.3913	3191.90	2.3896
8	34.5685	2.72449	54.3951	3191.90	2.5069
9	32.0269	2.81208	54.3990	3191.90	2.4584
10	28.8795	2.99576	54.4029	3191.90	2.4118

Table 4. Statistical description of inputs and output dataset.

Parameter	Min	Max	Average
GR	8.92	121.45	27.01
V_p (Km/s)	2.11	6.81	4.33
σ_v (Mpa)	54.37	70.54	62.46
RHOB (kg/m3)	1916.7	3191.9	2425.91
V_s (Km/s)	1.68	3.75	2.64

6. Prediction of Shear Wave Velocity Using ANFIS-ACO Models

In this research, hybrid ANFIS was utilized with ACO algorithm based on fuzzy c–means clustering and subtractive clustering. The ACO is combined with two ANFIS models (ANFIS–FCM and ANFIS–SCM) for determining the optimal value of its user–defined parameters. The optimization implementation by the ACO significantly improves the generalization ability of the ANFIS models. Related to the purpose, the selection of ACO parameters plays an important role in the optimization process. A single selection of ACO parameter has a tremendous effect on the rate of convergence. For this research, the optimal ACO parameters were determined by trial and error experimentations (Table 5). Furthermore, after 100 epochs of training, the optimal parameters of the ANFIS models estimated by the ACO are presented in Tables 6 and 7.

Table 5. Regulated parameters for run the ACO.

Parameter	Value
The number of ants (initial population)	20
Number of iterations	200
Pheromone intensity	100
Utility important factor	4
Evaporation important factor	1
Evaporation coefficient (ρ)	0.1
Initial value of the pheromone trail (τ)	100

These models were utilized to build a prediction model for the estimation of the Vs from available data, using MATLAB environment. A dataset that includes 4350 data points was employed in current study, while 3480 data points (80%) were utilized for constructing the model and the remaining data points (870 data points) were utilized for assessing the degree of accuracy and robustness.

Table 6. The optimal parameters of the ANFIS-FCM model estimated by the ACO.

Parameter	Value
Error goal of training	0.001
Initial step size	0.01
Step size decrease rate	2.1
Step size increase rate	3.1
Number of clusters	5

Table 7. The optimal parameters of the ANFIS-SCM model estimated by the ACO.

Parameter	Value
Error goal of training	0.001
Initial step size	0.01
Step size decrease rate	2.1
Step size increase rate	3.1
Influence radius of a cluster center	0.4

The training and testing procedures of two ANFIS-ACO models were conducted from scratch for the mentioned five datasets. The obtained MSE and R^2 values for training datasets indicate the capability of learning the structure of data samples, whereas the results of testing dataset reveal the generalization potential and the robustness of the system modeling methods. The characterizations of the ANFIS-ACO models are revealed in Table 8. As it can be seen in Table 8, Gaussian function plays the role of MF. The Gaussian membership function is popularly used in specifying fuzzy sets, which have the advantage of being smooth and differentiable at all points [23]. Furthermore, the Gaussian membership functions facilitate theoretical analysis of fuzzy systems, as they are continuously differentiable and infinitely differentiable, i.e. they have derivatives any grade [24].

Table 8. Characterizations of the ANFIS-ACO models for the estimation of the V_s.

Parameter	ANFIS-SCM improved by ACO	ANFIS-FCM improved by ACO
MF type	Gaussian	Gaussian
Output MF	Linear	Linear
Number of nodes	87	37
Number of linear parameters	40	15
Number of nonlinear parameters	64	24
Total number of parameters	104	39
Number of training data pairs	3330	3330
Number of testing data pairs	833	833
Number of fuzzy rules	8	3

The number of rules obtained for the ANFIS models (ANFIS-SCM and ANFIS-FCM) improved by ACO are 8 and 3 respectively. The MFs of the input parameters for different models are presented in Figures. 2 and 3.

Furthermore, correlations between measured and predicted values of V_s for training and testing phases are demonstrated in Figures 4 and 5. Also, a comparison between predicted values of V_s and measured values for data sets at training and testing phases is displayed in Figures 6 and 7.

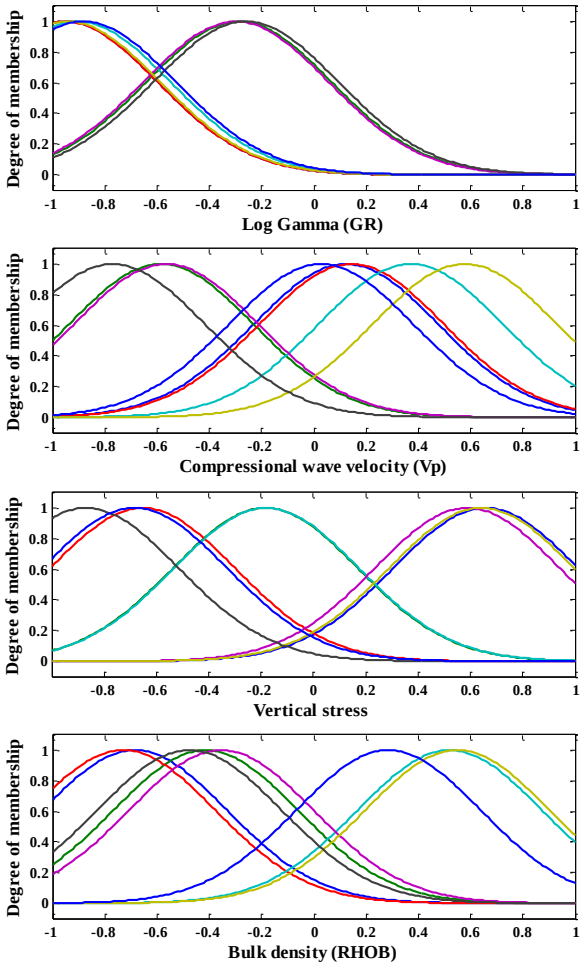

Figure 2. MFs obtained by ANFIS-SCM improved by ACO model.

As presented in Figures 6 and 7, the results of the ACO-improved ANFIS model compared to actual data demonstrate a good precision of this method. Furthermore, according to Figures 4 to 7, application of the ACO for the ANFIS optimization decreases the estimation error and increases correlation in all two states of using training and testing data.

7. Comparison among ANFIS-ACO Models and Empirical Correlations

In the latter stage of this study, a comparison among ANFIS-ACO models and empirical correlations [25,3,26,27,1,28] was performed. A List of empirical correlations used for estimating the V_s is shown in Table 9.

Different statistical concepts, including Mean Squared Error (MSE), variance account for (VAF) and correlation coefficient (R) were employed to carry out this comparison. Following equations demonstrate the aforementioned statistical tools:

$$MSE = \frac{1}{n}\sum_{i=1}^{n}(y_i - y_i')^2 \quad (15)$$

$$VAF = \left(1 - \frac{\mathrm{var}(y - y')}{\mathrm{var}(y)}\right) \quad (16)$$

$$R = \sqrt{1 - \frac{\sum_{i=1}^{n}(y_i - y_i')^2}{\sum_{i=1}^{n} y_i^2 - \frac{\sum_{i=1}^{n} y_i'^2}{n}}} \quad (17)$$

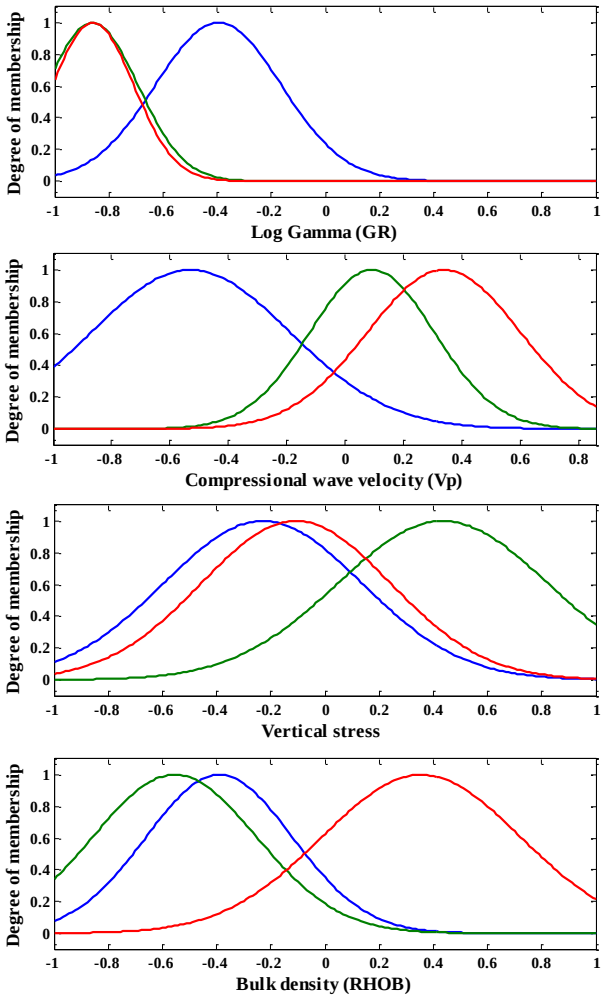

Figure 3. MFs obtained by ANFIS-FCM improved by ACO model.

While n is the number of samples, and y and y' are the measured and predicted values, respectively. Results of this comparison are shown in table 10. As it is obvious in table 10, ANFIS-SCM method enhanced by ACO outperformed other methods owing to higher R and VAF and lower MSE.

Table 9. List of empirical correlations used for estimating V_s.

Researcher	Empirical equation
F. Gassmann [28]	$V_s = 0.9131V_p + 0.2564$
G. R. Pickett [1]	$V_s = V_p / 1.9$
D.-h. Han et al. [27]	$V_s = 0.7936V_p - 0.7868$
J. P. Castagna, M. Backus [26]	$V_s = -0.05509V_p^2 + 1.0168V_p - 1.0305$
H. Eskandari et al. [3]	$V_s = -0.1236V_p^2 + 1.612V_p - 2.3057$
T. M. Brocher [25]	$V_s = 0.0064V_p^4 - 0.1238V_p^3 + 0.7949V_p^2 - 1.2344V_p + 0.7858$

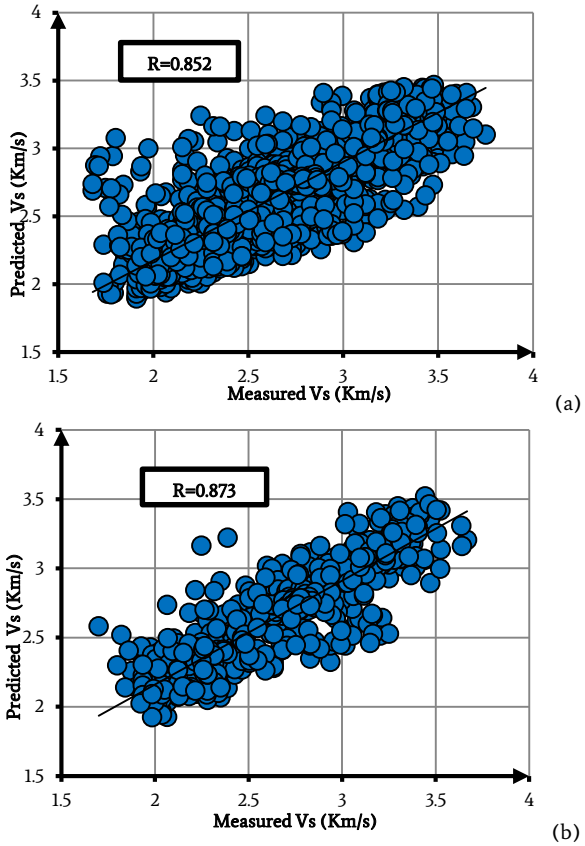

Figure 4. Correlation between measured and predicted values of V_s using ANFIS-SCM improved by ACO model a) training data, b) testing data.

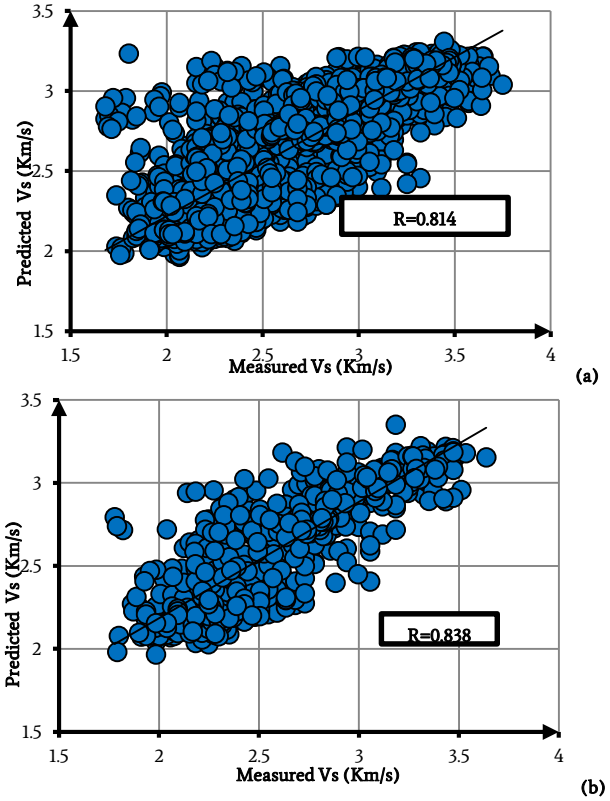

Figure 5. Correlation between measured and predicted values of V_s using ANFIS-FCM improved by ACO model a) training data, b) testing data.

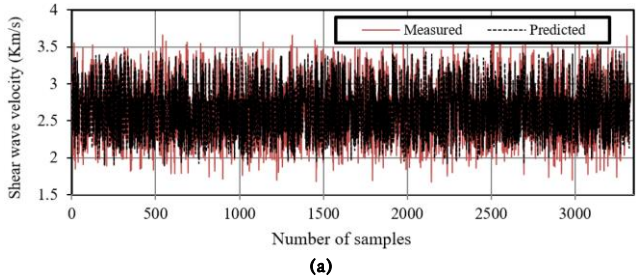

(a)

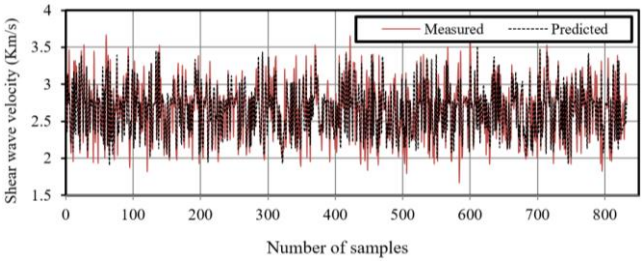

(b)

Figure 6. Comparison between measured and predicted values of V_s using ANFIS-SCM improved by ACO model a: training data, b: testing data.

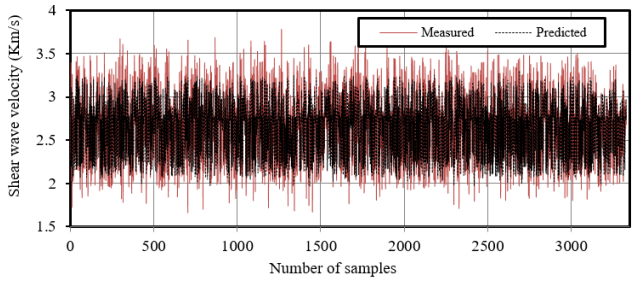

(a)

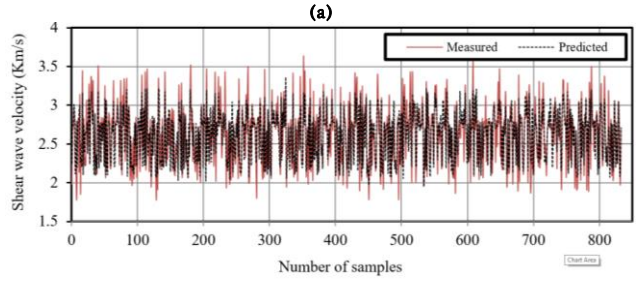

(b)

Figure 7. Comparison between measured and predicted values of V_s using ANFIS-FCM improved by ACO model a) training data, b) testing data.

Table 10. comparison of ANFIS-ACO models results with six well-known empirical correlations according to mean squared error (MSE), variance account for (VAF) and correlation coefficient (R).

Method		R	VAF	MSE
ANFIS-SCM improved by ACO	Training	0.852	72.70	0.0386
	Testing	0.873	76.32	0.0344
ANFIS-FCM improved by ACO	Training	0.814	66.27	0.0483
	Testing	0.838	70.37	0.0407
F. Gassmann [28]		0.742	-60.87	3.5692
G. R. Pickett [1]		0.762	60.63	0.0747
D.-h. Han et al. [27]		0.732	-6.27	0.1996
J. P. Castagna, M. Backus [26]		0.762	55.72	0.0703
H. Eskandari et al. [3]		0.767	46.45	0.1671
T. M. Brocher [25]		0.824	12.39	0.1268

8. Conclusions

A quantitative formulation between conventional well logs (available in all wells) and V_s eliminates the aforementioned problems and makes it possible to perform geophysical and geomechanical studies. Due to significance of calling for V_s knowledge, several researchers attempted to determine V_s through empirical correlations and/or traditional intelligent systems. Nonetheless, the quest for highest precision possible demands looking for high accuracy methods. In this study, hybrid ANFIS with ACO based on FCM and SCM was employed in order to respond this demand. ANFIS-ACO models were used to formulate conventional well log data, including Log Gamma (GR), V_p, vertical stress (σ_v) and bulk density (RHOB) into V_s. Results indicated ANFIS-ACO models performed acceptably and it was capable of mining hidden knowledge about V_s from conventional well logs. A total of 3030 data points from Marun reservoir of Iran was used for model construction and 833 data points were employed for assessment of ANFIS model results. A comparison between ANFIS-ACO models and previous works, including six well-known empirical correlations verified superiority of ACO-enhanced ANFIS-SCM model. The comparison showed ACO-improved ANFIS-SCM has a higher correlation coefficient and VAF and at the same time lower MSE. Finally, implementation of proposed methodology can produce V_s for old and/or cased holes where no shear wave measurement has been done. Applying ANFIS-ACO models for new wells can significantly reduce costs and bring about saves in time.

References

[1] Pickett G. R. (1963). Acoustic character logs and their applications in formation evaluation. Journal of Petroleum technology, 15 (06), 659-667.

[2] Eberli G. P., Baechle G. T., Anselmetti F. S., Incze M. L. (2003). Factors controlling elastic properties in carbonate sediments and rocks. The Leading Edge, 22 (7), 654-660.

[3] Eskandari H., Rezaee M., Mohammadnia M. (2004). Application of multiple regression and artificial neural network techniques to predict shear wave velocity from wireline log data for a carbonate reservoir South-West Iran. CSEG recorder, 42, 48.

[4] Rezaee M. R., Kadkhodaie Ilkhchi A., Barabadi A. (2007). Prediction of shear wave velocity from petrophysical data utilizing intelligent systems: An example from a sandstone reservoir of Carnarvon Basin, Australia. Journal of Petroleum Science and Engineering, 55 (3), 201-212.

[5] Rajabi M., Bohloli B., Gholampour Ahangar E. (2010). Intelligent approaches for prediction of compressional, shear and Stoneley wave velocities from conventional well log data: A case study from the Sarvak carbonate reservoir in the Abadan Plain (Southwestern Iran). Computers & Geosciences, 36 (5), 647-664.

[6] Moatazedian I., Rahimpour-Bonab H., Kadkhodaie-Ilkhchi A., Rajoli M. (2011). Prediction of shear and Compressional Wave Velocities from petrophysical data utilizing genetic algorithms technique: A case study in Hendijan and Abuzar fields located in Persian Gulf. Geopersia, 1 (1), 1-17.

[7] Asoodeh M., Bagheripour P. (2012). Prediction of compressional, shear, and stoneley wave velocities from conventional well log data using a committee machine with intelligent systems. Rock Mechanics and Rock Engineering, 45 (1), 45-63.

[8] Bagheripour P., Gholami A., Asoodeh M., Vaezzadeh-Asadi M. (2015). Support vector regression based determination of shear wave velocity. Journal of Petroleum Science and Engineering, 125, 95-99.

[9] Jang J. S. R. (1993). ANFIS: Adaptive-network-based fuzzy inference system. IEEE Transactions on Systems, Man and

Cybernetics, 23 (3), 665-685.

[10] Chiu S. L. (1994). Fuzzy model identification based on cluster estimation. Journal of intelligent and Fuzzy systems, 2 (3), 267-278.

[11] Bezdek J. C. (1973) Fuzzy mathematics in pattern classification. Cornell university, Ithaca

[12] Dorigo M., Blum C. (2005). Ant colony optimization theory: A survey. Theoretical computer science, 344 (2), 243-278.

[13] Socha K., Dorigo M. (2008). Ant colony optimization for continuous domains. European journal of operational research, 185 (3), 1155-1173.

[14] Toksari M. D. (2006). Ant colony optimization for finding the global minimum. Applied Mathematics and Computation, 176 (1), 308-316.

[15] Kanan H. R., Faez K., Taheri S. M. (2007) Feature selection using ant colony optimization (ACO): a new method and comparative study in the application of face recognition system. In: Advances in Data Mining. Theoretical Aspects and Applications. Springer, pp 63-76

[16] Xu D., Fu L. Ant Colony Optimization and its Applications. In: Intelligent Systems and Applications, 2009. ISA 2009. International Workshop on, 2009. IEEE, pp 1-4

[17] Zeng D. H., Liu Y., Jiang L. B., Li L., Xu G. A New Approach to Cutting Temperature Prediction Using Support Vector Regression and Ant Colony Optimization. In: Advanced Engineering Forum, 2012. Trans Tech Publ, pp 145-152

[18] Gorjian M., Memarian H., Moosavi M., Mehrgini B. (2012). Dynamic properties of anhydrites, marls and salts of the Gachsaran evaporitic formation, Iran. Journal of Geophysics and Engineering, 10 (1), 015001.

[19] Rolf B., Mohammed W., Mohsen P. (2006). A preliminary study of casing collapse in Iran Hydroquest Report. Schlumberger Oil Company.

[20] Wang Z. (2001). Fundamentals of seismic rock physics. Geophysics, 66 (2), 398-412.

[21] Cabello P., Falivene O., López-Blanco M., Howell J., Arbués P., Ramos E. (2010). Modelling facies belt distribution in fan deltas coupling sequence stratigraphy and geostatistics: The Eocene Sant Llorenç del Munt example (Ebro foreland basin, NE Spain). Marine and Petroleum Geology, 27 (1), 254-272.

[22] Sfidari E., Kadkhodaie-Ilkhchi A., Rahimpour-Bbonab H., Soltani B. (2014). A hybrid approach for litho-facies characterization in the framework of sequence stratigraphy: A case study from the South Pars gas field, the Persian Gulf basin. Journal of Petroleum Science and Engineering, 121, 87-102.

[23] Babuška R. (2012) Fuzzy modeling for control, vol 12. Springer Science & Business Media.

[24] Shin Y. C., Xu C. (2008) Intelligent systems: modeling, optimization, and control, vol 30. CRC press.

[25] Brocher T. M. (2005). Empirical relations between elastic wavespeeds and density in the Earth's crust. Bulletin of the Seismological Society of America, 95 (6), 2081-2092.

[26] Castagna J. P., Backus M. (1993). AVO analysis-tutorial and review. Offset-dependent reflectivity: theory and practice of AVO analysis, 3-36.

[27] Han D.-h., Nur A., Morgan D. (1986). Effects of porosity and clay content on wave velocities in sandstones. Geophysics, 51 (11), 2093-2107.

[28] Gassmann F. (1951) Elasticity of porous media: Über die Elastizität poröser Medien: Vierteljahrsschrift der Naturforschenden Gesselschaft in Zurich. Heft.